

## Damping wide-area oscillations in power systems: a model predictive control design

Emrah BIYIK<sup>1,\*</sup>, Munir HUSEIN<sup>2</sup>

<sup>1</sup>Department of Energy Systems Engineering, Faculty of Engineering, Yaşar University, İzmir, Turkey

<sup>2</sup>School of Electrical Engineering, Kookmin University, Seoul, Korea

Received: 21.05.2017

Accepted/Published Online: 21.11.2017

Final Version: 26.01.2018

**Abstract:** Electromechanical oscillations in power systems have been observed ever since synchronous generators were interconnected to provide reliability and higher generation capacity, and they have become a severe threat for the safe and economic operation of modern interconnected power grids. To dampen these oscillations, wide-area damping controllers (WADCs) have been introduced by utilizing wide-area measurement systems and synchronized phasor measurement units. In this paper, we present a systematic approach for designing WADCs using a model predictive control (MPC) technique to damp interarea oscillations in the power system. The MPC controller computes optimal control signals for the excitation system of a remote generator where it will supplement the local power system stabilizers that are used as damping controllers. The performance of the proposed approach has been assessed on the IEEE 16-generator 68-bus test system, and it is shown that the interarea oscillations can be effectively and robustly damped under varying operation conditions.

**Key words:** Power systems, model predictive control, interarea oscillations, wide-area damping, phasor measurement unit, optimization

### 1. Introduction

For stable and secure power system operation, the damping of electromechanical oscillations between interconnected generators is of immense importance [1]. If not damped out quickly, these oscillations may result in line tripping, network splitting, generator outages, and even blackouts [2]. The electromechanical oscillations that pose a threat to the power system can be characterized in two main groups: local mode and interarea mode. Oscillations with frequencies of 0.7 to 2.0 Hz [3] are specified as local mode, and they occur when a generator is oscillating against the remainder of the system. The characteristics of these oscillations are well understood and solutions to their stability problems are available.

Interarea mode oscillations, however, are between a group of generators, and they occur in the frequency range of 0.1 to 0.7 Hz [3]. The characteristics of these modes are far more complex to analyze and control. Heavy power transfer across weak tie-lines or high-gain exciters are the main cause of interarea oscillations [3]. Multiple dominant interarea modes are commonly observed in large power systems. These modes exist because of the dynamics of power transfer and they are associated with groups of generators oscillating against each other. The interarea mode oscillations hamper the power transfer capacity of the regions containing the groups of coherent generators [4].

\*Correspondence: emrah.biyik@yasar.edu.tr

Unstable oscillations caused by interarea modes have been commonly observed in actual power systems [5,6], including the 2003 blackout in the United States and Canada, where a severe oscillation of 0.4 Hz [7] brought down an entire power system. The traditional control approach in use today to damp these oscillations is to employ classical local power system stabilizers (PSSs). These devices are effective in damping local modes by supplementing control action through the generator excitation system. PSSs have limited effectiveness in damping interarea modes, because these controllers are single-input single-output, use local inputs, and are not coordinated [8]. These local controllers make use of a linear model with fixed parameters and capture the system behavior around a particular operating point. Thus, these conventional local controllers are usually valid around only this point. However, power systems exhibit dynamically varying generation and load characteristics in a wide operating space. In addition, some operating conditions may render the interarea mode uncontrollable and/or unobservable from a particular area [9]. This leads the local PSSs to lack observation of interarea modes and hence become ineffective in damping that mode. Recently, wide-area control systems (WACSs) have been gaining attention in effective damping of interarea oscillations. The recent advancements in wide-area measurement systems (WAMSs) [10,11] use phasor measurement units (PMUs), which are based on a global positioning system and provide accurate and time-synchronized measurement of crucial power system variables such as angle, frequency, voltage, and current. Therefore, the WAMS enables development of WACSs that rely on such data.

A WACS usually requires some form of a WAMS communication link between generators and the control station to collect system data and broadcast control signals [12]. The operational flexibility provided by the WACS typically justifies the installation of a WAMS. Early wide-area damping controllers (WADCs) were designed in [9], and it was concluded that when wide-area signals are coupled with local controllers, the transient performance of the power system can be improved against the interarea oscillations. In [13], the authors proposed a hierarchical wide-area control structure, where wide-area control signals are added to local PSS signals to dampen both local and interarea modes. Tuning of the multilayer controller structure was posed as a sequential optimization problem. In [14], a linear matrix inequality was formulated to synthesize a mixed  $H_2/H_\infty$  output-feedback controller for wide area damping.

In this paper, we develop a model predictive control (MPC) approach [15] for damping wide-area oscillations. MPC is suitable for the wide-area problem thanks to its ability to handle multivariable systems with constraints in a systematic way. Several other applications of MPC in wide-area control have been reported in the literature [16,17]. The major limitation in those applications, however, is their large computational load due to large state-space models. As a result, their slow optimization time may limit their applicability to fast power systems dynamics. In this paper, however, we derive the input-output prediction model equations offline and obtain a fast optimization solution. Thus, we can employ a detailed power system model to capture the system dynamics more accurately while obtaining optimal results fast.

The organization of the paper is as follows: Section 2 states the problem formulation, while Section 3 gives details of the MPC wide-area control design. Simulation results are presented in Section 4, followed by concluding remarks in Section 5.

## 2. Problem formulation

In power systems, the synchronous generators serve as the primary source of electrical energy. The stable operation of the power system also relies on other components including excitation systems, governors, power system stabilizers, and the loads. The main objective of the controllers designed for power system stability is to

ensure robust synchronization of the interconnected generators. In this paper, we used a sixth-order subtransient model for the generator, as described in [3]. The nonlinear equations that describe the generator rotor angle, speed, and power dynamics are as follows:

$$\dot{\delta} = \omega - \omega_s, \quad (1)$$

$$J\dot{\omega} = T_m - T_e - \hat{D}(\omega - \omega_s), \quad (2)$$

$$\tau\dot{E} = -\frac{x_d}{x'_d}E + \frac{x_d - x'_d}{x'_d}V \cos(\delta - \theta) + E_F, \quad (3)$$

$$P^G = \frac{E \times V}{x'_d} \sin(\delta - \theta) + \left( \frac{x'_d - x_q}{2x_q x'_d} \right) V^2 \sin(2(\delta - \theta)), \quad (4)$$

$$Q^G = \frac{E \times V}{x'_d} \cos(\delta - \theta) - \left( \frac{x'_d - x_q}{2x_q x'_d} \right) (1 - \cos(2(\delta - \theta))), \quad (5)$$

where  $\delta$  is the rotor angle,  $\omega$  is rotor frequency,  $\omega_s$  is the synchronous frequency,  $J$  is the moment of inertia,  $T_m$  is the mechanical torque,  $T_e$  is the electromechanical torque,  $\hat{D}$  is the damping coefficient,  $E$  is the quadrature-axis internal emf,  $P^G$  and  $Q^G$  the active and reactive power of the generator, and  $V$  and  $\theta$  are the voltage and phase at the generator bus. The details of the generator parameters, the regulating devices (exciter, governor, PSS), and the loads are omitted due to lack of space and the reader is referred to [3] for details. The overall model including the synchronous generator along with the associated regulating devices has 15 state variables for each synchronous machine.

Our objective in this paper is to develop an optimal control strategy to damp the interarea oscillations as quickly as possible after a disturbance. In other words, we want to achieve convergence of the generator rotor frequency  $\omega$  to the synchronous frequency  $\omega_s$  to prevent excessive power swings across the network. We achieve this by adding a supplementary MPC control signal on top of the existing PSS (through the  $T_e$  signal), as described in the next section.

### 3. MPC wide-area control design

#### 3.1. MPC wide-area damping controller architecture

In a typical power system, local PSSs perform well in damping local oscillation modes, while they have limited performance in handling interarea mode oscillations. Thus, the damping of these interarea oscillations should be increased by a wide-area controller. The wide-area controller utilizes wide-area measurements and that provides a supplemental signal to the local PSS. Figure 1 illustrates the MPC wide-area control scheme that is used in this paper.

In real time, critical signals that capture the state of the system are measured by PMUs and are sent to the MPC controller via the WAMS. These state measurements,  $\hat{x}(t)$  are collected at discrete measurement times  $\Delta t$ . If a particular signal is not available, a state estimator would normally be needed. The MPC then predicts the system evolution with the help of its dynamic model, computes the optimal control signals ( $u$ ) over a chosen control horizon  $N_c$ , and sends these signals to each generator excitation system.

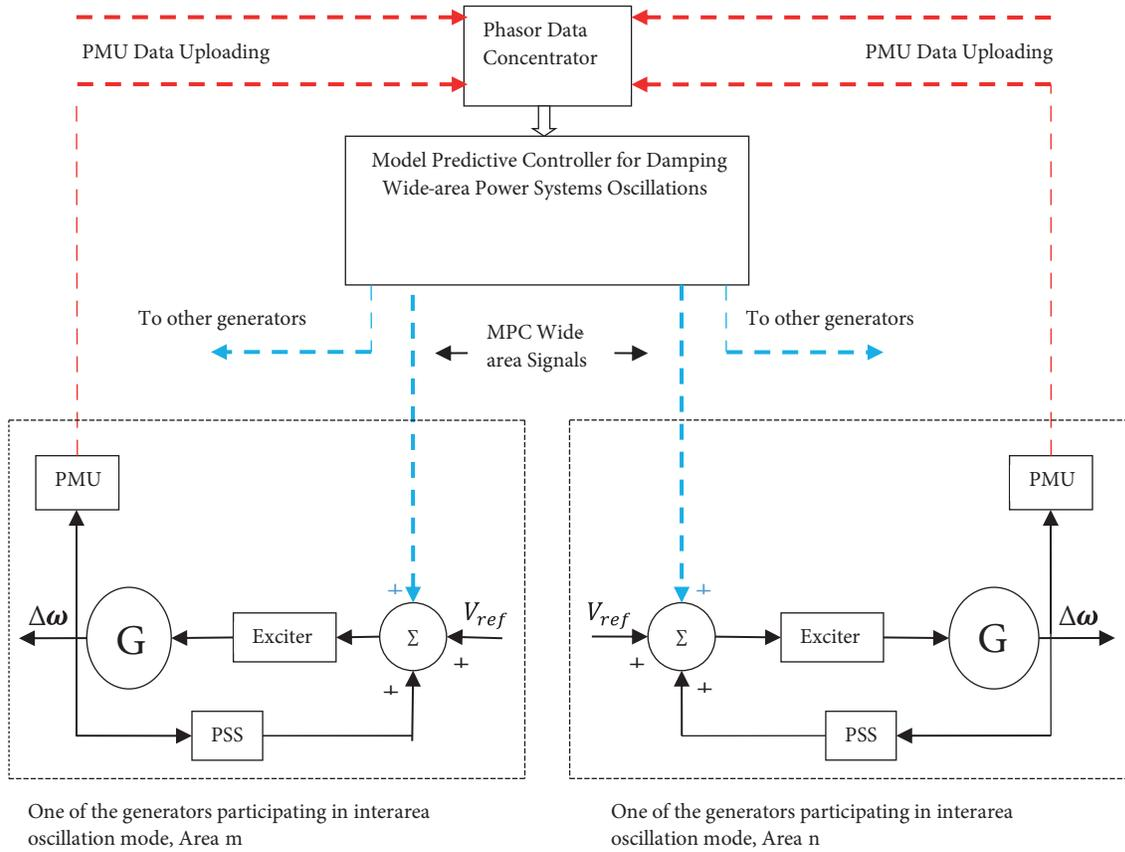


**Figure 1.** Architecture of MPC wide-area damping control system.

The operation of the MPC controller is described as follows. At every control step, data from measurements (or from state estimation algorithms) are acquired to obtain the most current representation of system dynamics. A system model is then called repeatedly to predict the dynamics and constraints within a time window of several minutes, while a constrained optimization problem is solved to obtain the optimal actuator set-points that minimize the defined objective, and is compliant with the operating constraints within the prediction window. Then the first set of the optimal set-point values is sent as a reference to the actuators. Finally, a new set of measurements is acquired and the whole process is repeated for the subsequent control steps. These steps are illustrated in Figures 2 and 3.

### 3.2. Controller Synthesis

The power system is modeled with the MATLAB Power System Toolbox (PST). Time-domain simulations are done with the `s_simu` package in the PST, while small signal stability analysis package `svm_mgen` from the PST is used to linearize the full-order model described in Section 2. The continuous time linear model can shown as:

$$\dot{x} = A_c x + B_c u, \tag{6}$$

$$y = C_c x, \tag{7}$$

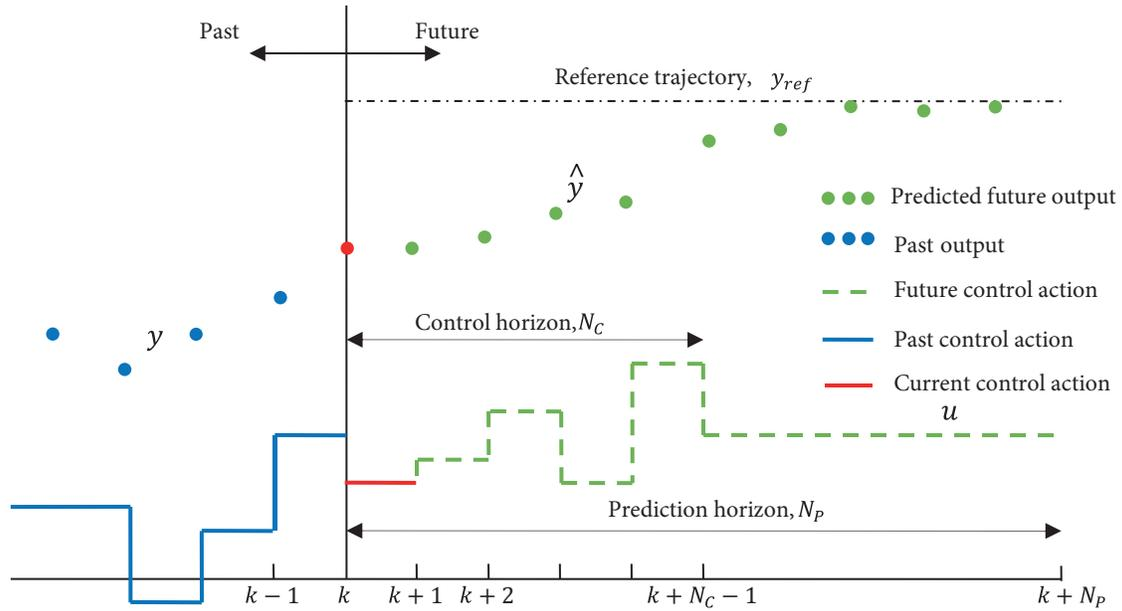


Figure 2. Basic model predictive control strategy.

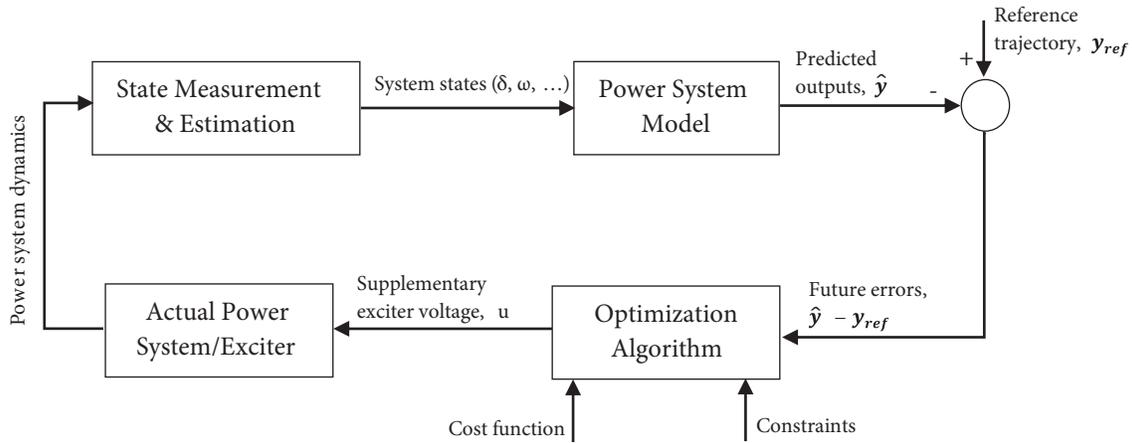


Figure 3. Structure of the model predictive controller.

where  $x \in R^{m_x}$ ,  $u \in R^{m_u}$ , and  $y \in R^{m_y}$  are the state, input, and output vectors, respectively. In our design, the MPC wide-area signals are added to each generator excitation system as a supplementary control input  $u = [u_1 \ u_2 \ u_3 \ \dots \ u_n]$ , where  $n$  is the number of generators controlled by the MPC controller. Eqs. (6) and (7) are then discretized using a sufficiently small time step ( $\Delta t = 0.1$  s in our case) to obtain the discrete-time dynamics:

$$x[k + 1] = Ax[k] + Bu[k], \tag{8}$$

$$y[k] = Cx[k]. \tag{9}$$

At time  $k$ , a measurement (or estimation) of the current system state  $\hat{x}(k)$  is obtained. Next, by using  $\hat{x}(k)$  as the initial state, Eqs. (8) and (9) are iterated  $N_p$  times, where  $N_p$  is the MPC prediction horizon, to compute

a prediction of the output sequence  $\hat{y}[k]$  as in Eqs. (10) and (11) below:

$$X[k] = P_x \hat{x}[k|k] + P_u u[k-1] + P_{\Delta u} \Delta U[k], \quad (10)$$

$$Y[k] = P_y X[k] = P_y P_x \hat{x}[k|k] + P_y P_u u[k-1] + P_y P_{\Delta u} \Delta U[k], \quad (11)$$

where,

$$P_x = \begin{bmatrix} A \\ A^2 \\ \vdots \\ A^{N_P} \end{bmatrix}, \quad P_u = \begin{bmatrix} B \\ AB + B \\ \vdots \\ \sum_{i=0}^{N_P-1} A^i B \end{bmatrix}, \quad P_y = \begin{bmatrix} C & 0 & \cdots & 0 \\ 0 & C & \cdots & 0 \\ \vdots & \vdots & \ddots & \vdots \\ 0 & 0 & \cdots & C \end{bmatrix},$$

$$P_{\Delta u} = \begin{bmatrix} B & 0 & 0 \\ AB + B & B & 0 \\ \vdots & \vdots & \vdots \\ \sum_{i=0}^{N_C-1} A^i B & \sum_{i=0}^{N_P-1} A^i B & B \\ \vdots & \vdots & \vdots \\ \sum_{i=0}^{N_C-2} A^i B & \sum_{i=0}^{N_P-2} A^i B & \sum_{i=0}^{N_P-N_C} A^i B \end{bmatrix}.$$

Based on the above closed-form prediction equations (Eqs. (10) and (11)), our MPC controller computes the predicted state and output trajectory very fast. Given a particular cost function to minimize, the optimal input sequence  $\hat{u}[k+i|k]$  is then computed while satisfying Eqs. (10) and (11) as constraints. In the MPC control scheme, we have two main objectives. First, we want the output signal to follow a reference trajectory, and secondly we want to achieve this with minimal change input signals so as to avoid large input oscillations. To this effect, the cost function we use in this paper is given in Eq. (12) below:

$$J[k] = \sum_{i=0}^{N_p-1} \|\hat{y}[k+i+1|k] - y_{ref}[k+i+1|k]\|_{W_{y_i}}^2 + \sum_{i=0}^{N_C-1} \|\Delta \hat{u}[k+i+1|k]\|_{W_{\Delta u}}^2. \quad (12)$$

The mismatch between the output  $\hat{y}[k+i+1|k]$  and the desired reference output trajectory  $y_{ref}[k+i+1|k]$  as well as the variation in input sequence  $\Delta \hat{u}[k+i+1|k]$  is penalized. In general, the reference trajectory may be some predetermined trajectory fed to the controller by the system operator.

There are quite a number of successful optimization packages that can solve the quadratic programming problem stated in Eq. (12). In this paper, we employ the MATLAB platform. At time step  $k$ , the control input sequence  $\hat{u}[k+i|k]$  is obtained as the solution of the optimization problem. The first entry in this control sequence ( $\hat{u}[k|k]$ ) is sent to the excitation system of the generators for implementation. At the next time step  $k+1$ , the state of the system is measured (or estimated) as  $\hat{x}(k+1)$ , the optimization is repeated with this new updated state information, and the cycle continues.

**Remark** Tuning of the MPC design parameters is of immense importance for a well-posed optimization problem and a satisfactory controller performance [18]. The prediction horizon,  $N_P$ , should be selected to include all significant dynamics; otherwise, the performance may be poor and important events may be unobserved. The prediction horizon should be greater than the control horizon and the settling time combined. Increasing the control horizon,  $N_C$ , makes the controller more aggressive and increases computational effort; typically,

$5 \leq N_C \leq 20$  is suggested in the literature [18]. The control horizon should capture the anticipated transient duration. The weighting matrices  $W_y$  and  $W_{\Delta u}$  are typically diagonal with the largest elements corresponding to the most important variables. In the output weighting matrix  $W_y$ , the most important variables should be given the largest weights. In the input weighting matrix (move suppression matrix)  $W_{\Delta u}$ , increasing the values of weights tends to make the MPC controller more conservative by reducing the magnitudes of the input moves. Thus, increasing  $W_{\Delta u}$  slows down the response but enhances transient oscillations.

#### 4. Simulation results

We test our MPC controller on the IEEE 16-machine, 68-bus test system as shown in Figure 4. Generators G1 to G9 represent the New England Test System (NETS) while generators G10 to G13 represent the generation of the New York Power System (NYPS). Three neighboring areas connected to the NYPS are represented by G14 to G16. All the generators use a subtransient model, with local power system stabilizers installed on G1 to G12 with rotor speeds as input.

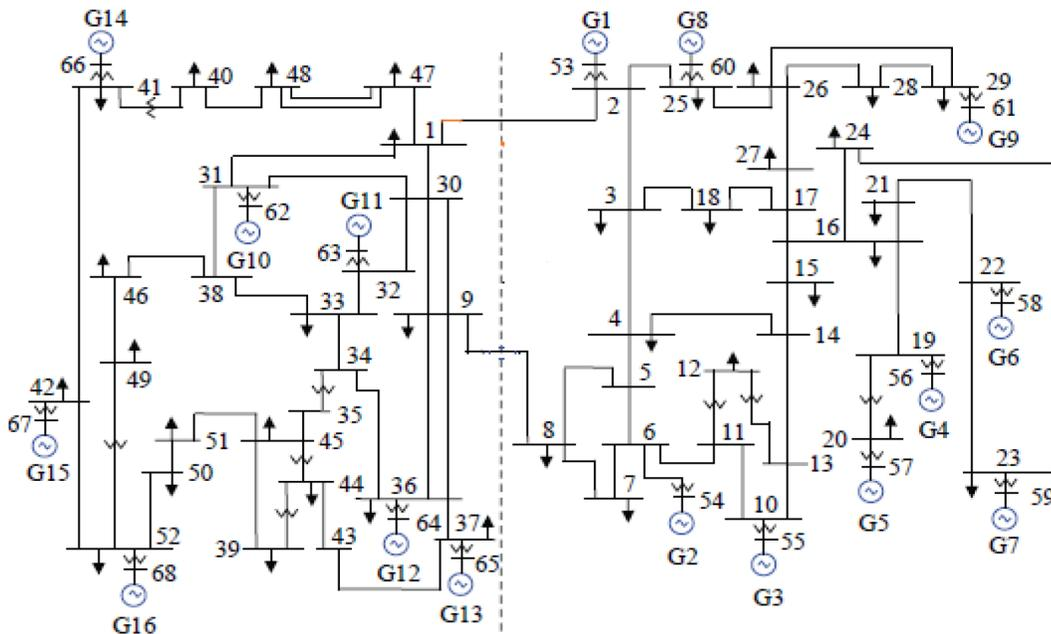


Figure 4. IEEE 16-generator 5-area test system.

##### 4.1. Full-order model and small signal analysis

Generators 1 to 12 have 15 states while generators 13 to 16 have 9 states, bringing the total number of generator states to 216. There are 33 states for active load modulation and another 33 for reactive load modulation, which brings the total number of states for the whole test system to 282. The small signal analysis reveals that there exist few local and interarea modes with damping ratio less than 5%. Figure 5 shows the plot of frequency against damping ratio of the system's modes.

As shown in Table 1, modes 1 and 2 are interarea modes while modes 3, 4, and 5 are local modes. Note that local modes appear even though PSSs were installed. This is a typical behavior of very large and complicated power systems. Because these modes have large frequencies, however, they will decay quickly. Thus, their effect is not of concern despite their low damping ratios, and supplementary damping to these modes is not necessary.

**Table 1.** Classification of electromechanical oscillation for modes shown in Figure 5.

Mode index	Mode type	Frequency (Hz)	Damping ratio
1	Interarea	0.4618	0.0479
2	Interarea	0.6634	0.0268
3	Local	0.9759	0.0223
4	Local	1.0523	0.0398
5	Local	1.2868	0.0321
6	Local	1.8079	0.0490

The eigenvector associated with a mode indicates the relative change in the states that would be observed when the mode of oscillation is excited. Figure 6 shows the compass plot of rotor angle terms of the interarea mode eigenvector and confirms that mode 1 (0.4618 Hz) is an interarea mode, since aggregate generators in areas 3, 4, and 5 are oscillating against generators in areas 1 and 2. We thus conclude from small signal analysis that our test system has 2 lightly damped interarea modes of  $0.1392 \pm j2.9016$  and  $-0.1118 \pm j4.1638$  with frequencies of 0.4618 Hz and 0.6634 Hz, respectively.

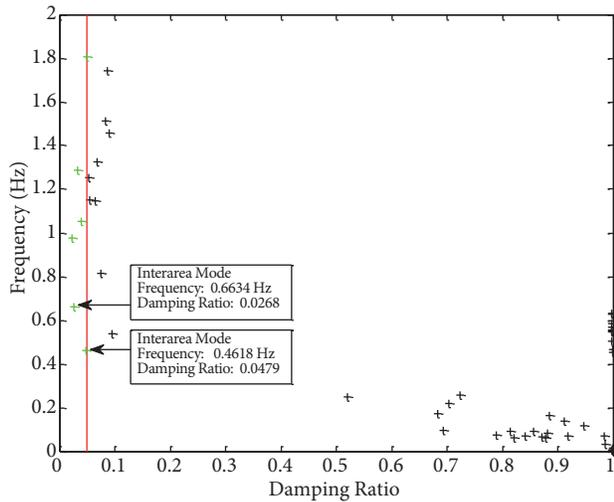


**Figure 5.** Calculated modes of IEEE 16-generator 5-area test system.

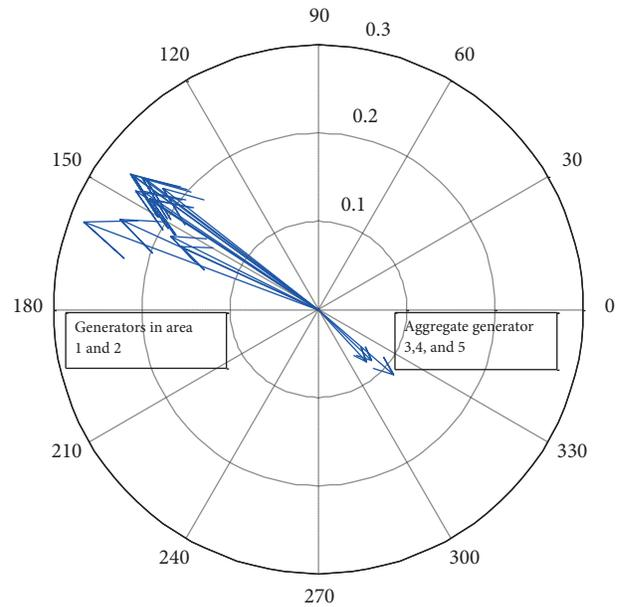


**Figure 6.** Compass plot of rotor angle terms of interarea (0.4618 Hz) mode eigenvector.

#### 4.2. Controller synthesis

The dynamic model used in MPC has 282 state variables ( $x$ ) and 16 output variables ( $y$ ) of angular speeds, with reference  $y_r$  ( $= 1$  pu). The control signal  $u$  comprises 12 supplementary inputs to the excitation system of generators G1 to G12. Constraints are imposed on the control signal  $u$  as  $-0.1 \leq u \leq 0.1$ . These constraints were imposed on the MPC wide-area signal to avoid an excessive interference between wide-area damping control and the local control provided by PSS. For the proposed MPC controller, the desired response was achieved

by setting the control parameters as in Table 2. Note that the weights of output signals to generators 13 to 16 are set to zero because MPC signals were not sent to these generators since they are a group of aggregated generators.

**Table 2.** MPC design parameters.

Variable	Description	Value
$\Delta t$	Sampling interval	0.1
$N_P$	Prediction horizon	75
$N_C$	Control horizon	10
$W_u$	Weights on manipulated variables	0.01
$W_{\Delta u}$	Weights on manipulated variable rates	0.1
$W_y$	Weights on the output signal of G1 to G12	10
$W_y$	Weights on the output signal of G13 to G16	0

### 4.3. Simulation results

The performance of the MPC controller is tested under the following two disturbance scenarios: 1) an impulse signal at the input mechanical torque of generator 12, and 2) an impulse signal applied to the exciter reference voltage of generator 12.

**Simulation scenario 1:** In Scenario 1, an impulse type disturbance signal is applied to the mechanical torque of generator 12. Figure 7 shows the response for over a period of 25 s. When the MPC controller is not present, slowly damped oscillations are observed.

Next, the response with the MPC controller active is shown in Figure 8. A comparison between Figures 7 and 8 shows that the MPC controller is effective in damping the interarea oscillations and reduces the settling time to 8 s. The supplementary control signals sent by the MPC controller to the excitation system of generators 1, 2, 11, and 12 are shown in Figure 9. Today's electrical grid is typically equipped with high bandwidth communication between power plants and the central grid operator. In addition, the exciter systems

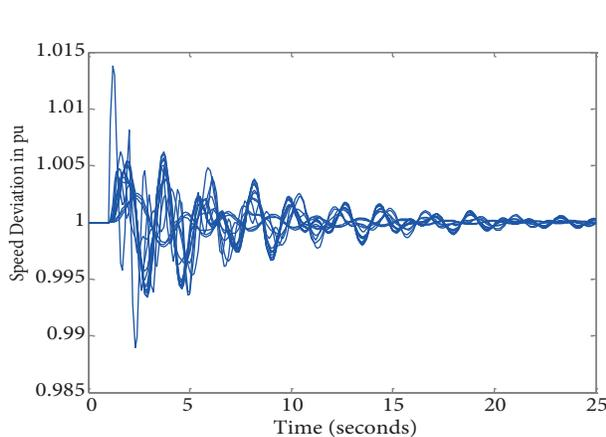


**Figure 7.** Speed deviation of all generators with only PSS, no MPC (Scenario 1).

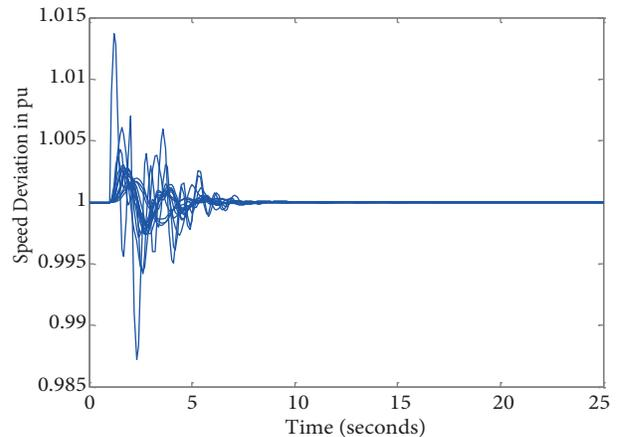


**Figure 8.** Speed deviation of all generators with MPC controllers (Scenario 1).

in the generators work on subsecond time scales and can generate and actuate fast variations in the exciter voltages with high resolution. Even though Figure 9 suggests fast time scales and continuous values in input dynamics, the present infrastructure has the capacity to implement the supplementary input signals as in Figure 9. Figure 10 shows the speed deviation of generator 1 with and without MPC WADC and clearly reveals the improved performance by the proposed MPC wide-area controller.

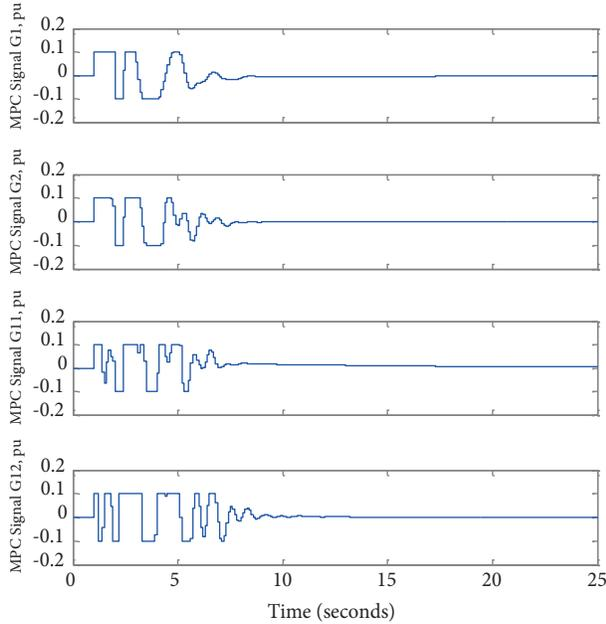


**Figure 9.** MPC wide-area signals to G1, G2, G11, and G12 (Scenario 1).

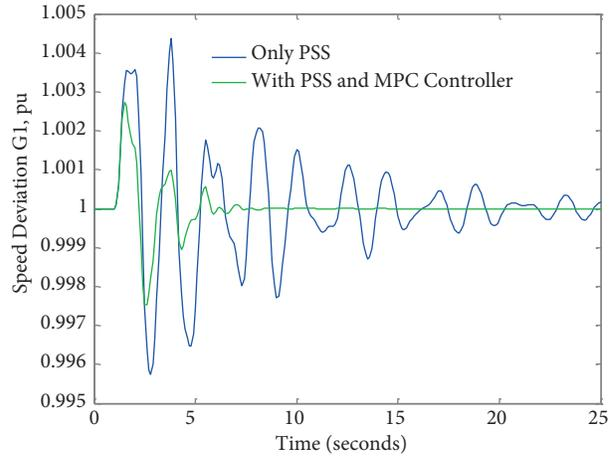


**Figure 10.** Speed deviation of generator 1 (Scenario 1).

**Simulation scenario 2:** In this case scenario, the disturbance used is an impulse signal applied to the exciter reference voltage of generator 12 (Figure 4) in order to excite the interarea oscillations. Figure 11 shows the simulated response over a period of 25 s. When no MPC wide-area controller is used, a sustained, slowly

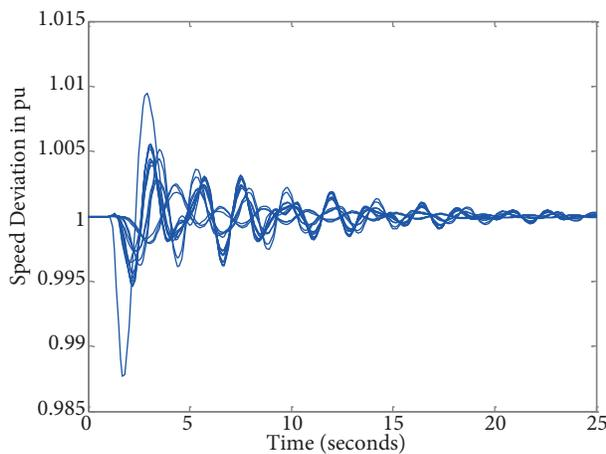


**Figure 11.** Speed deviation of all generators with only PSS, no MPC (Scenario 2).

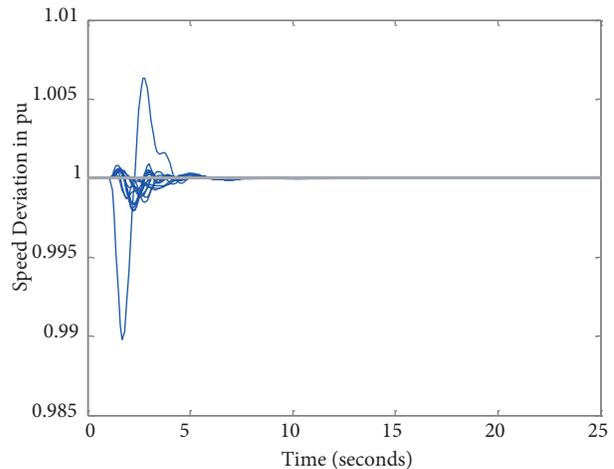


**Figure 12.** Speed deviation of all generators with MPC controller (Scenario 2).

damped oscillation is observed. Next, the same MPC wide-area controller of case scenario 1 was introduced in order to investigate the robustness of the designed controller; Figure 12 shows a response over a period of 25 s. Compared with the system response without MPC controller (Figure 11), it is observed that the MPC WADC damps the interarea oscillations efficiently (settling time is reduced to approximately 5 s). This proves that the designed controller is robust and can damp oscillations generated by a variety of disturbances.

## 5. Conclusions

In this paper a systematic procedure of designing a WADC using the MPC technique to damp interarea oscillations in a power system is presented. At each control time step, the controller solves a quadratic programming problem to compute an optimal input sequence and then sends these signals to the excitation system of a remote generator, where it will supplement the local damping controllers. Power system stabilizers were used as local damping controllers in this paper. The effectiveness and robustness of the proposed MPC controller for a wide-area damping scheme have been verified on the IEEE 16-generator 68-bus test system. Simulation results reveal that the proposed controller effectively damps interarea oscillations under varying operating conditions and different disturbances.

## Acknowledgment

We would like to thank the anonymous reviewers, whose comments and suggestions significantly helped us improve the quality of the paper. The work of the first author was supported in part by the Building Controls project funded by the European Commission (H2020-MSCA-IF-2015, grant agreement no: 708984).

## References

- [1] Klein M, Rogers GJ, Kundur P. A fundamental study of inter-area oscillations in power systems. *IEEE T Power Syst* 1991; 6: 914-921.
- [2] Rogers G. *Power System Oscillations*. Norwell, MA, USA: Kluwer Academic Publishers, 2000.
- [3] Kundur P. *Power System Stability and Control*. New York, NY, USA: McGraw-Hill, 1994.
- [4] Zhou EZ. Application of static VAR compensators to increase power system damping. *IEEE T Power Syst* 1993; 8: 655-661.
- [5] Taylor C, Erickson D, Martin E, Venkatasubramanian V. WACS – Wide-area stability and voltage control system: R&D and online demonstration. *P IEEE* 2005; 93: 892-906.
- [6] Breulman H, Grebe E, Losing M, Winter W, Witzman R, Dupuis P, Houry MP, Margotin T, Zerenyi J, Dudzik J. Analysis and damping of inter-area oscillations in the UCTE/CENTREL power systems. In: *CIGRE 2000*; Paris, France.
- [7] Chadwick JE. How a smarter grid could have prevented the 2003 U.S. cascading blackout. In: *IEEE 2013 Power and Energy Conference at Illinois*; 22–23 February 2013; Champaign, IL, USA. New York, NY, USA: IEEE. pp. 65-71.
- [8] Klein M, Rogers GJ, Moorthy S, Kundur P. Analytical investigation of factors influencing power system stabilizers performance. *IEEE T Power Syst* 1992; 7: 382-388.
- [9] Aboul-Ela ME, Sallam AA, McCalley JD, Fouad AA. Damping controller design for power system oscillations using global signals. *IEEE T Power Syst* 1996; 11: 767-773.

- [10] Mittelstadt WA, Krause PE, Overholt PN, Hauer JF, Wilson RE, Rizy DT. The DOE wide-area measurement system (WAMS) project - demonstration of dynamic Information technology for future power system. In: Fault and Disturbance Analysis & Precise Measurements in Power Systems Conference; 8–10 November 1995; Arlington, VA, USA. pp. 1-8.
- [11] Phadke AG. Synchronized phasor measurements – a historical overview. In: IEEE/PES Transmission and Distribution Conference and Exhibition 2002: Asia Pacific; 6–10 October 2002; Yokohama, Japan. New York, NY, USA: IEEE. pp. 476-479.
- [12] Tomsovic K, Bakken DE, Venkatasubramanian V, Bose A. Designing the next generation of real-time control, communication, and computations for large power systems. P IEEE 2005; 93: 965-979.
- [13] Kamwa I, Grondin R, Hebert Y. Wide-area measurement based stabilizing control of large power systems – a decentralized/ hierarchical approach. IEEE T Power Syst 2001; 16: 136-153.
- [14] Zhang Y, Bose A. Design of wide-area damping controllers for inter-area oscillations. IEEE T Power Syst 2008; 23: 1136-1143.
- [15] Maciejowski JM. Predictive Control with Constraints. Harlow, UK: Prentice Hall, 2002.
- [16] Wang D, Glavic M, Wehenkel L. A new MPC scheme for damping wide-area electromechanical oscillations in power systems. In: 2011 IEEE PES PowerTech Conference; 19–23 June 2011; Trondheim, Norway. New York, NY, USA: IEEE. pp. 1-7.
- [17] Wang L, Cheung H, Hamlyn A, Cheung R. Model predictive adaptive control of inter-area oscillations in multi-generator power system. In: 2009 IEEE PES General Meeting; 26–30 July 2009; Calgary, Canada. New York, NY, USA: IEEE. pp. 1-7.
- [18] Rossiter JA. Model-Based Predictive Control: A Practical Approach. Boca Raton, FL, USA: CRC Press, 2004.